75 Yousaf, M. N., Mrksich, N. (1999) Diels-Alder reaction for the selective immobilization of protein to electroactive self-assembled monolayers. *J. Am. Chem. Soc.* **121**, 4286–4287.
76 Bunimovich, Y., Ge, G., Beverly, K. C., Ries, R. S., Hood, L., Heath, J. R. (2004) Electrochemically programmed, spatially selective biofunctionalization of silicon wires. *Langmuir* **24**, 10630–10638.
77 Curreli, M., Li, C., Sun, Y. H., Lei, B., Gundersen, M. A., Thompson, M. E., Zhou, C. W. (2005) Selective functionalization of In2O3 nanowire mat devices for biosensing applications. *J. Am. Chem. Soc.* **127**, 6922–6923.
78 Rohde, R., Agnew, H., Yeo, W.-S., Bailey, R., Heath, J. R. (2006) A non-oxidative approach towards chemically and electrochemically biofunctionalizing Si(111). *J. Am. Chem. Soc.* **128**, 9518–9525. DOI: 10.1021/ja062012b.
79 Star, A., Gabriel, J. C. P., Bradley, K., Gruner, G. (2003) Electronic detection of specific protein binding using nanotube FET devices. *Nano Lett.* **3**, 459–463.
80 Wang, W. U., Chen, C., Lin, K.-H., Fang, Y., Lieber, C. M. (2005) Label-free detection of small-molecule–protein interactions by using nanowire nanosensors. *Proc. Natl. Acad. Sci. USA* **102**, 3208–3212.
81 Chen, R. J., Bangsaruntip, S., Drouvalikis, K. A., Kam, N. W. S., Shim, M., Li, Y., Kim, W., Utz, P. J., Dai, H. (2003) Noncovalent functionalization of carbon nanotubes for highly specific electronic biosensors. *Proc. Natl. Acad. Sci. USA* **100**, 4984–4989.
82 Star, A., Gabriel, J.-C. P., Bradley, K., Gruner, G. (2003) Electronic detection of specific protein binding using nanotube FET devices. *Nano Lett.* **3**, 459–463.

13
Bionanoarrays

Rafael A. Vega, Khalid Salaita, Joseph J. Kakkassery, and Chad A. Mirkin

13.1
Overview

Patterned arrays of biomolecules, such as DNA, proteins, viruses, and cells, have been utilized as powerful tools in a variety of biological studies. Microarrays, in particular, have led to significant advances in many areas of medical and biological research, opening up avenues for the combinatorial screening and identification of single-nucleotide polymorphisms (SNPs), high-sensitivity expression profiling of proteins, and high-throughput analysis of protein function [1]. With the advent of powerful new nanolithographic methods, such as dip-pen nanolithography (DPN) [2], there is now the possibility of reducing the feature size in such arrays to their physical limit, the size of the structures from which they are made of, and the size of the structures they are intended to interrogate (Figure 13.1) [3]. Such massive miniaturization not only allows one to increase the density of combinatorial libraries, to increase the sensitivity of such structures in the context of a biodiagnostic event, and to reduce the required sample analyte volume, but also to carry out studies that are not possible with the more conventional microarray format. Arrays with features on the nanometer-length scale open up the opportunity to study many biological structures at the single particle level [4]. Such features can be used to immobilize and orient individual virus particles and to study many important processes such as cell infectivity and virus proliferation and transmission. These miniaturized features allow one to contemplate the creation of the equivalent of an entire combinatorial library (e.g., a gene chip or complex protein array) underneath a single cell, thus opening new possibilities for the study of important fundamental, multivalent, processes such as cell-surface recognition, adhesion, differentiation, growth, proliferation, and apoptosis.

In this chapter, methods for preparing biological nanoarrays made from biomaterials – including proteins, oligonucleotides, and viruses – will be high-

Nanobiotechnology II. Edited by Chad A. Mirkin and Christof M. Niemeyer

ISBN: 978-3-527-31673-1

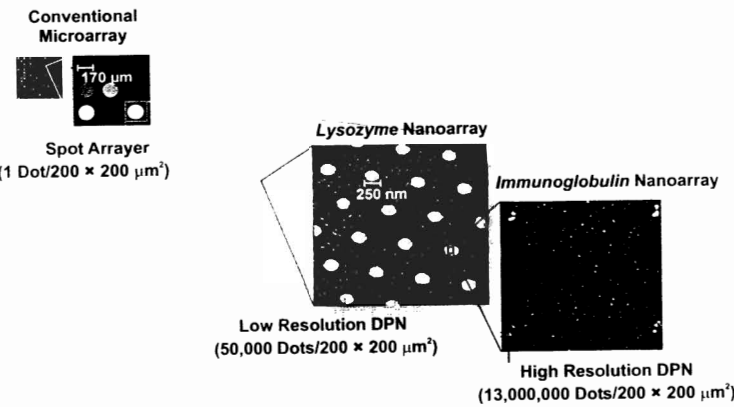

Fig. 13.1 Using low-resolution dip-pen nanolithography (DPN), 55 000 protein spots, each of 250 nm, can be spotted in an area occupied by a single spot (200 μm diameter) in a conventional microarray. Patterns can be further miniaturized using high-resolution DPN to generate a total of 13 000 000 spots in a 200 × 200 μm^2 area. (Figures reprinted with permission from Ref. [3]; © 2005, American Chemical Society.)

lighted. The focus will be on techniques that allow feature size to be controlled on the sub-500 nm length scale.

13.2 Methods

There is currently a suite of techniques available – with various advantages and disadvantages – for generating nanoscale features of biological molecules. The goal of this section is to highlight some of the more promising methods for generating nanoarrays of biological molecules, and to emphasize how they differ in terms of resolution, multiplexing capabilities, and throughput.

13.2.1 Atomic Force Microscope-Based Methods

Since its inception in 1986, atomic force microscopy (AFM) has been used for elucidating structural details for a variety of surface-bound molecules and materials [5]. Recently, AFM-based lithographies have emerged as powerful tools for patterning biological molecules at the nanometer length scale, most notably through the invention of DPN [4, 6, 7]. In this section, the use of AFM-based methods for generating arrays of biological molecules will be introduced and highlighted.

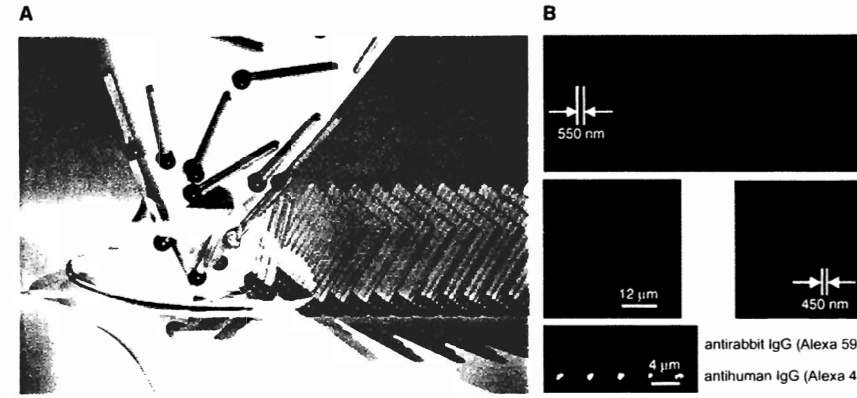

Fig. 13.2 (A) Schematic diagram depicting the dip-pen nanolithography (DPN) process. (B) Fluorescence images of DPN-generated antibody structures on a negatively charged SiO_2 surface. (Part B reprinted with permission from Ref. [13]; © 2003, Wiley-VCH.)

Most AFM-based patterning techniques use a scanning probe tip to selectively eliminate (i.e., etch, electrochemically oxidize, or displace) part of an adsorbed monolayer to generate a template for capturing biomolecules [8–10]. An exception to this method is DPN, where an "ink"-coated AFM tip is used to directly deliver nanoscopic amounts of an adsorbate to a surface on the sub-50 nm to many micrometer-length scale [2, 11] (Figure 13.2). DPN is particularly well-suited for patterning biological and soft organic structures onto surfaces, as it operates under ambient conditions without the need for an electron or ion beam [11]. Also, because DPN is a "constructive" rather than "destructive" patterning tool, the fabrication of high-density combinatorial arrays of different biomolecules with ultrahigh registry is possible. Thus far, DPN has been used to generate arrays of synthetic DNA oligomers, proteins, and peptides [6, 7, 12–19]. In many cases, tip and substrate modification protocols have been developed to maintain the biological fidelity of the deposited structures [12].

The direct deposition of biomolecules using DPN requires the chemical modification of an AFM tip for reproducible tip coating, and the implementation of suitable ink–substrate coupling chemistries for reliable biomolecular transport. For example, the direct deposition of DNA was achieved using hexanethiol-modified oligonucleotides on gold surfaces, and acrylamide-modified oligonucleotides on oxidized silicon wafers that had been pre-modified with 3′-mercaptopropyltrimethoxysilane [7]. The biological activity of the resulting patterns was confirmed by hybridization with fluorophore- or nanoparticle-labeled oligonucleotides (Figure 13.3).

DPN has been used to generate chemical affinity templates for the adsorption of proteins, DNA, and even more recently virus particles from solution [4, 6, 20–

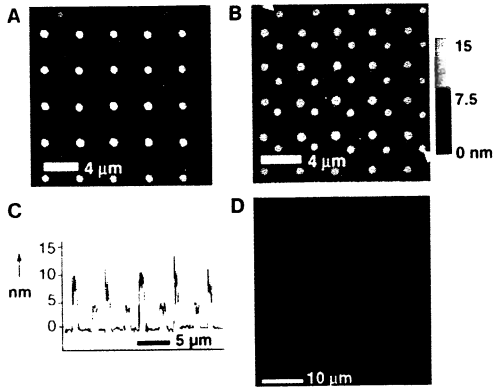

Fig. 13.3 Direct patterning of multiple-DNA molecules by DPN. (A) Combined red-green fluorescence overlay image of two different fluorophore-labeled sequences (Oregon Green 488-X and Texas Red-X) simultaneously hybridized to a two-sequence array deposited on a silanized SiO_x substrate by DPN. (B) Tapping-mode atomic force microscopy (AFM) image of 5-nm (dark) and 13-nm (light) -diameter gold NPs assembled on the same pattern after dehybridization of the fluorophore-labeled DNA. (C) A line plot was taken diagonally through both NP patterns, and the start and finish are indicated by the white arrows in (B). (D) Dark-field optical image showing scattering from densely packed 13 nm-diameter DNA-functionalized NPs hybridized to a 1600-dot DNA array patterned on SiO_x. (Parts A–C reprinted with permission from Ref. [7]; © 2003, American Association for the Advancement of Science.)

24]. Indirect patterning approaches are best suited for generating single-component nanoarrays, and can be used without having to optimize a unique set of conditions for the deposition of different classes of biomolecules. How such arrays can be used to study cell-surface recognition is highlighted in Section 13.3.4.

Other AFM-based methods can be used to indirectly pattern DNA and protein nanostructures. These methods rely on a localized tip–surface interaction to eliminate selected areas in an adsorbed monolayer, which in turn allows for another group of molecules to adsorb to these patterned areas. Liu and coworkers [8, 25, 26] have demonstrated that nanografting can be used to generate nanoscale patterns of DNA and proteins, respectively. In nanografting, a scanning probe tip under a high applied load displaces resist molecules within a self-assembled monolayer, which then allows solution species to adsorb to these exposed sites. Lines of DNA, as narrow as 10 nm, have been fabricated using this technique [25].

In a similar approach, Cai and coworkers [9] demonstrated that a conductive AFM tip can be used to selectively eliminate parts of a monolayer on a silicon (Si) substrate. They then used these substrate-exposed areas to immobilize avidin and biotinylated bovine serum albumin (BSA). Matsui and coworkers [10] showed

that an AFM tip could be used to "shave" parts of an octadecanthiol monolayer on Au to subsequently fill and immobilize antibodies into these areas. This shaving technique has been used to generate two-component arrays of antibodies (mouse and human IgGs), and the biological activity of such structures was confirmed by reacting them with the corresponding fluorophore-labeled secondary antibodies. The difficulty of this serial process comes from the cross-reactivity and nonspecific binding of the antibodies. The first set of features is always exposed to the solution used to generate the second set of features. Furthermore, feature size-broadening often results from tip damage, and the approach, thus far, has not been amenable to parallelization, which imposes significant throughput limitations.

Overall, AFM-based patterning techniques provide a resolution commensurate with the size of certain individual biomolecules and structures (~10 nm), offering new opportunities to investigate biological reactions, and to investigate mono- and multivalent processes at the single particle level (for discussions, see Sections 13.3 and 13.5). Such uses cannot be addressed using microarrays, because of a size mismatch between the features in the array and the structures being probed (e.g., viruses, cells, and spores). Although indirect elimination-based techniques – such as nanografting, nanoshaving, or nanoscale oxidation – provide excellent resolution, these techniques are currently limited in throughput and do not offer extended multiplexing capabilities. At present, only DPN is capable of the direct delivery of multiple biomolecules at ultrahigh resolution and registry. Furthermore, recent advances in parallel DPN using linear [27] and large two-dimensional (2-D) arrays of cantilevers [28] have substantially increased the throughput of this method, and this now allows researchers to pattern over square-centimeter areas.

13.2.2
Nanopipet Deposition

Nanopipetting is based on scanning ion-conductance microscopy (SCIM), which was a technique developed to scan soft non-conducting materials by using an electrolyte-filled micropipet as a probe [29]. In SCIM, the ionic-current flowing between an electrode inside the micropipet and a counterelectrode inside the bath is used to control the pipet–substrate distance. By using a pipette with a 100- to 150-nm diameter orifice, research groups have used SCIM to deliver small quantities of DNA and proteins onto various substrates (Figure 13.4) [30]. The number of molecules exiting the tip orifice is dependent on a combination of applied current, electro-osmotic flow, electrophoresis, and dielectrophoresis, depending on the size, charge, and polarizablity of the specific molecules being deposited. It is therefore necessary to characterize the delivery of molecules from the pipet experimentally, as each molecule type has different transport properties that depend upon the magnitude of the electric field.

SCIM deposition of biomolecules occurs in solution, and consequently the feature size depends heavily on the pipet–substrate distance and on the diffusion of

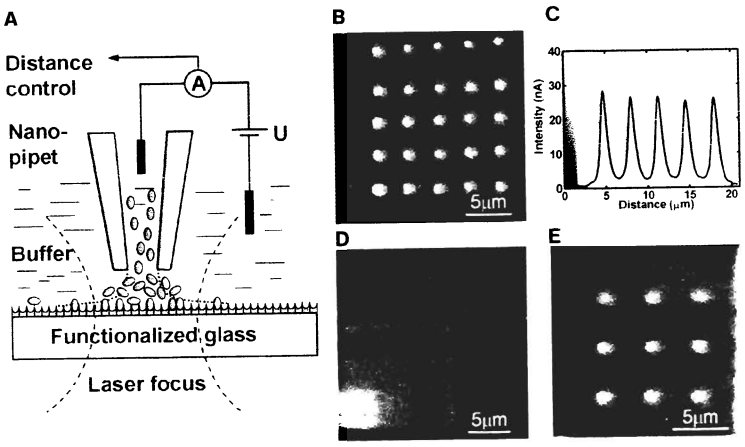

Fig. 13.4 (A) Schematic of a typical nanopipet experiment. Fluorescence images (B) 25 dots of biotinylated DNA deposited with a 10-s hold time each onto a streptavidin-coated glass surface. (C) Line scan of the bottom row in part (B); the FWHM is 830 ± 80 nm. (D) Squares of biotinylated DNA written over each other to create a pattern with increasing intensities. (E) Dots of protein G on a positively charged glass surface. (Reprinted with permission from Refs. [30, 31]; © 2002 and 2003, American Chemical Society.)

biomolecules to the surface. Once the molecules leave the nanopipet tip, there are two contributions to their motion toward the surface: (i) the directed electroosmotic flow from the pipet; and (ii) subsequent diffusion in solution on the substrate. The highest resolution achieved by nanopipet deposition thus far is approximately ~800 nm. As the deposition occurs in a buffered solution, the biological activity of the deposited molecules is typically preserved [31].

More recently, Klenerman and coworkers [32] reported a "double-barreled nanopipet", where two types of molecules are independently delivered to a surface from the pipet barrels of a single tip. This technique can be carried out in air, which provides higher resolution and eliminates the registry problems involving the deposition of two different species on a surface. This method has been used to deposit spots of DNA or proteins as small as ~500 nm onto a polyethyleneimine (PIE)-coated glass substrate.

Nanopipet-based delivery of biomolecules is among the few techniques capable of directly depositing biomolecules onto surfaces but, at present, it is significantly limited in terms of resolution and throughput.

13.2.3 Beam-Based Methods

Electron-beam lithography (EBL) is a technique widely used to fabricate nanoscale masks in the semiconductor industry [33], and it is capable of producing

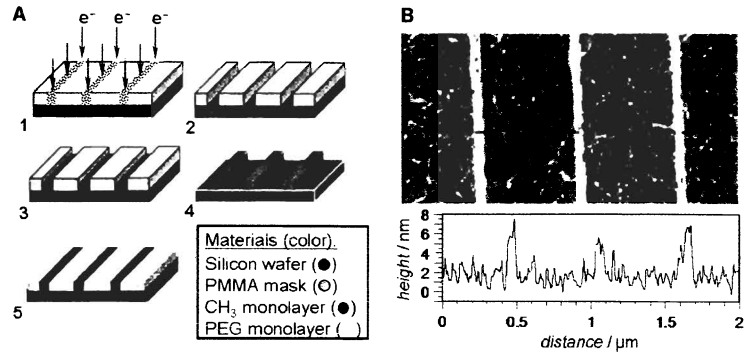

Fig. 13.5 (A) Schematic diagram of the five steps associated with the fabrication of anisotropic chemical nanopatterns. 1, Irradiation of a poly(methyl methacrylate) (PMMA) resist layer, spin-coated on a silicon wafer, with a focused electron beam to create a pattern of parallel lines. 2, Selective dissolution of the irradiated PMMA. 3, Grafting of the methyl-terminated alkylsilanes on bare silicon oxide. 4, Dissolution of the remaining PMMA. 5, Grafting of PEG-alkylsilanes on bare silicon oxide. (B) AFM height image (2 × 1 μm^2), in air, of a CH_3-50/PEG-550 area after collagen adsorption where the cross-section is taken along the horizontal black-dashed line. (Reprinted with permission from Ref. [37]; © 2005, Wiley-VCH.)

high-quality sub-10 nm features on inorganic substrates. Recently, it has been used to generate nanoscale arrays of biomolecules via an indirect patterning approach. With EBL, patterns are first drawn on a thin layer of photoresist or on a chemisorbed monolayer of molecules. Patterned areas are then chemically modified to capture biomolecules present in a bulk solution, and the surrounding areas are passivated with other molecules that resist the nonspecific adsorption of biomolecules [34–36].

For example, Dupont-Gillain and coworkers [37] generated collagen nanoarrays using EBL. They initially wrote thin lines (line widths = 30–90 nm) in a poly(methyl methacrylate) (PMMA) resist, which was selectively dissolved to allow for the gas-phase grafting of a CH_3-terminated alkylsilane (Figure 13.5A). Collagen molecules can then adsorb onto these CH_3-terminated alkylsilane features. The group then showed that collagen can be aligned and assembled into continuous bundles when the feature size is much smaller than the length of one collagen molecule (~300 nm) (Figure 13.5B). Jonas and coworkers [38] also studied the adsorption of globular proteins onto nanoscopic CH_3-terminated line templates surrounded by chemisorbed oligo(ethylene oxide). The group demonstrated that the orientation of the adsorbed globular proteins can be tailored by reducing the size of the adsorption region below 50 nm, which is believed to reorient the proteins adsorbed at the edges of each stripe. Both of these examples demonstrate that EBL can be used to generate templates that adsorb biomolecules and, in some cases, control their orientation. However, this approach is limited with respect to multiplexing, because only one type of biomolecule can be depos-

ited on a nanostructured array. Although parallel EBL methods are currently being developed, these are prohibitively complex, and thus the throughput of EBL based patterning is also quite limited [33].

In order to address the issue of low-throughput in EBL, the use of nanoimprint lithography (NIL) was introduced for patterning biomolecules [39, 40]. NIL typically replicates EBL-defined structures in polymer films, and can be used to rapidly generate extremely small features over large areas. Various proteins such as streptavidin and anti-catalase were immobilized onto aminosilane patterns as small as 75 nm. The biological activities of the immobilized proteins were confirmed by monitoring their reaction with fluorophore-labeled antibodies. However, NIL is also an indirect approach to patterning biomolecules, and therefore it is difficult to pattern multiple biomolecules in the context of a single nanoarray. NIL, thus far, can only replicate pre-existing patterns, and therefore each pattern requires the design and fabrication of a different mask, which can be prohibitive if one needs systematically to modify the pitch, size, and/or pattern shape. For certain applications, these parameters are important, and will be discussed in Section 13.3.4.

13.2.4
Contact Printing

Microcontact printing (μCP) techniques have been utilized over the past decade to generate micron-scale biomolecule patterns on a variety of substrates [41]. More recently, nanocontact printing (nCP) techniques have been developed for the direct or indirect deposition of a variety of biomolecules on the sub-50 nm length scale [42–44]. μCP and nCP rely on the use of an elastomeric stamp patterned with relief structures to generate patterns and structures with feature sizes ranging from 30 nm to 100 μm.

By decreasing the feature size on an elastomeric poly(dimethylsiloxane) (PDMS) stamp to below 100 nm and using dilute protein ink solutions, Delamarche and coworkers [42] demonstrated that a very small number of green fluorescent protein molecules (GFP) can be patterned on a glass substrate. The exact position of the GFP molecules is within ±50 nm of the theoretical center of the dots, although there is a significant fraction (~60%) of surface sites that remain unoccupied. Huck et al. [43] utilized a combination of "sharp" and "hard" PDMS stamps, with high-molecular weight inks to generate 60-nm multimeric protein lines. The advantage of using nCP is that it is a direct-write technique and therefore a much simpler method for generating nanoscale arrays of biomolecules compared to indirect methods such as EBL or NIL. Similar to NIL, nCP can be used to pattern over large areas, although pattern registry and pattern size can vary depending on the uniformity of the applied load on the stamp. The ability to deposit multi-component structures in nCP or μCP is quite limited, but DPN has recently been used to ink individual stamp features; it has also been demonstrated that three different DNA strands can be patterned simultaneously [44].

Recently, a novel DNA stamping technique – sometimes referred to as supramolecular nano-stamping (SuNS) – was introduced independently by our group [45], Crooks et al. [46] and Stellacci et al. [47, 48] for the efficient replication and printing of DNA micro- and nanoarrays. SuNS consists of three steps: hybridization; contact; and dehybridization. SuNS has allowed the printing of DNA patterns as small as 50 nm on PMMA substrates, and may prove to be a simple method for rapidly replicating DNA arrays. This method, which shows promise for printing chemically modified DNA, relies on the highly specific and selective hybridization properties of oligonucleotides. The throughput of this technique is very high, although each new pattern requires the use of a new mask.

13.2.5
Assembly-Based Patterning

Periodic nanoarrays of biomolecules have been prepared via three different approaches that use three different classes of materials: colloidal particles [49, 50]; diblock copolymer micelles [51]; and 2-D DNA tiles [52, 53]. In each of these cases, a phase-separated material or prefabricated structure is used to direct the assembly of biomolecules into a preconceived periodic pattern. Directed-assembly techniques are viewed as attractive methods by some researchers because they are often straightforward to implement, inexpensive, and in some cases provide very high resolution. For example, nanosphere lithography (NSL) utilizes the interstitial spaces in a monolayer of close-packed colloidal particles to pattern a variety of materials. NSL provides hexagonally patterned lithographic masks for further surface processing. For example, Ocko et al. [54] have used 300-nm colloidal particles of polystyrene to protect an underlying vinyl monolayer from oxidation and subsequent chemical coupling to polyethylene glycol (PEG)-silane. This approach was used to generate ~120 nm islands that could capture lysozyme proteins from solution, and the biological activity of patterned lysozyme was subsequently confirmed using antibody–antigen binding. Although NSL is limited to hexagonal patterns of single-component structures with modest control over array architectural dimensions (feature size and pitch), this method offers an economical solution for large-scale high-resolution protein patterning. It should be noted that Van Duyne and coworkers have conducted some impressive NSL studies with biological systems and have dramatically extended the flexibility and capabilities of the approach [55, 56]. It is conceivable that some of their advances could be extended to biological systems [57].

Spatz and coworkers [51] have shown that the assembly of diblock copolymer micelles on glass surfaces results in the formation of a hexagonal, close-packed structure. When gold (Au) nanoparticles (NPs) are enclosed within these micelles, hexagonally packed Au NPs form on glass substrates once the organic polymer is removed by plasma treatment. The distances between the Au NPs can be adjusted through the choice of diblock-copolymer size, and were varied between 28 ± 5, 58 ± 7, 73 ± 8, and 85 ± 9 nm. Such structures were used to study

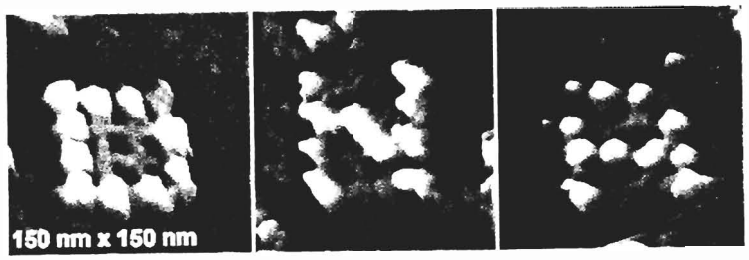

Fig. 13.6 Demonstration of precise programming by assembly. The letters "D, N, and A" were assembled on DNA tile arrays (4 × 4) decorated with protein using the two-step minimal depth strategy. (Reprinted with permission from Ref. [59]; © 2006, Wiley-VCH.)

the activation of integrin function (this is described in more detail in Section 13.3.4). This is an interesting approach towards controlling the spacing between ligands, although the range of inter-particle spacings is limited.

Recently, periodic arrays of assembled DNA tiles or grids have been used as elaborate scaffolds to organize materials at the nanometer-length scale [52, 53, 58, 59]. DNA assemblies have been formed using carefully designed linear oligonucleotides with complementary base-pairing segments that form branch-junction motifs. These DNA assemblies were produced with various geometrical structures and functions, ranging from periodic one-dimensional (1-D) materials to three-dimensional (3-D) polyhedra. The precise positioning of a single streptavidin protein by site-selective attachment within finite 2-D DNA grids is shown in Figure 13.6. The synthesis of such nanostructures involves interactions between a large number of short oligonucleotides, and the final yield is highly dependent on the stoichiometry. Although the length scale over which these arrays are regular is small (~1 μm) and the precise position of each DNA assembly cannot be controlled or macroscopically addressed, these arrays provide nanometer precision in controlling the spacing between materials.

13.3
Protein Nanoarrays

Protein microarrays have enabled the high-throughput analysis of protein function, protein–protein interactions, catalysis, drug screening, and other biochemical reactions [1, 60]. However, biorecognition is inherently a nano- rather than a microscopic phenomenon. Therefore, nanoarrays are beginning to enable scientists not only to ask but also answer some detailed questions regarding the interactions of biological structures (i.e., cells) with immobilized protein features [51]. Furthermore, nanoarrays of proteins (i.e., antibodies) with well-defined feature size and spacing have been shown to be important and advantageous in developing novel immunoassay schemes for the sensitive and selective detection of macromolecules [20]. In this section, we will describe the immobilization chemistries used to prepare protein nanoarrays, and some of the applications of these arrays.

13.3.1
Strategies for Immobilizing Proteins on Nanopatterns

Because there are many types of proteins with a wide variety of functional groups, different chemical methods have been designed to effectively immobilize the different classes of proteins. Proteins are extremely fragile, contain multiple domain structures, and can have multiple interaction sites. One of the simplest and fastest ways to immobilize proteins is through electrostatic interactions. However, proteins immobilized in this way are often not robust and can be significantly affected by changes in solution pH and ionic strength, thereby allowing for the possibility of protein desorption. Because there is no specific interaction between the desired protein and the surface, the proteins are often randomly attached to such substrates. In the case of microarrays, electrostatic binding, in many cases, results in immobilized proteins with an acceptable level of target binding. This is because the feature size is large enough such that some of the immobilized proteins are in the proper orientation to support analyte binding. Nanoarrays are not likely to perform the same as the feature area is significantly reduced in size [6, 12, 61], and in order to realize a system with feature properties that are similar from spot to spot, immobilization strategies that result in uniform protein immobilization with consistent and optimized bioactivity are needed.

Certain covalent attachment strategies offer researchers the ability to generate immobilized protein structures with substantially higher bioactivities. These techniques have been commonly used in array-type formats to permanently fix proteins on a substrate through a variety of functional groups present on their surface, such as amino-, carboxyl-, hydroxyl-, and thiol-moieties. These moieties can be readily coupled to an amine- or thiol-terminated surface with the appropriate crosslinkers [60]. The covalent approach, usually, produces higher concentrations of proteins on the patterned area than what is produced through electrostatic adsorption. However, the proteins are still immobilized in random forms, which can lead to decreased sensitivities and complete loss of biological activity in surface-based immunoassays compared to immobilization strategies that orient the proteins [62, 63].

A variety of techniques have been developed for the directed immobilization of proteins – specifically antibodies – in active states. The most common method has been the use of antibody-binding proteins A, G, and A/G, which bind the F_c portions of antibodies, leaving their F_{ab} binding sites exposed to solution. Researchers have coupled the covalent approach, described above, for the immobilization of protein A/G to direct the immobilization of antibodies on a surface [64, 65]. However, protein A/G is costly and has varying affinities – and in some cases no affinity – for the different classes of antibodies, and this limits their use in some immunobased assays. Recently, a new approach has been developed in our

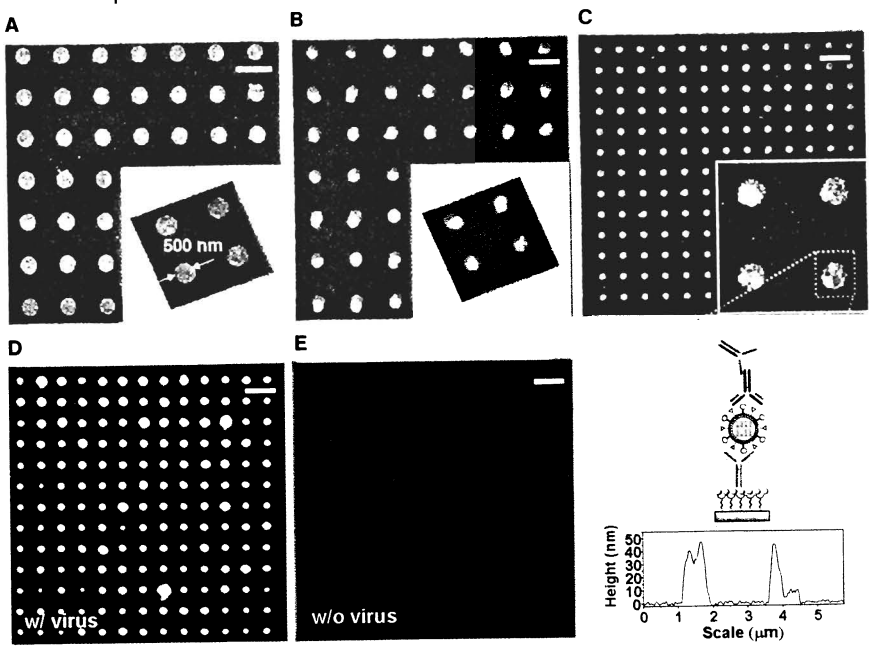

Fig. 13.7 AFM tapping mode image of (A) anti-Udorn (polyclonal goat IgG) immobilized on 500-nm MHA dot arrays pretreated with $Zn(NO_3)_2 \cdot 6H_2O$; (B) after the addition and binding of the influenza virus; and (C) followed by the sandwiching of the virus-antibody complex through anti-HA (monoclonal mouse IgG1) and goat anti-mouse (secondary antibody). Fluorescence images of (C) treated with (D) and without (E) influenza virus particles. Scale bars: A, B = 1 μm; C–E = 3 μm for the array and 1 μm for the insert. (Reprinted with permission from Ref. [24]; © 2006, Wiley-VCH.)

group that uses metal-ions as a linker between the surface and the antibody [24]. This approach has the potential to be a low-cost alternative for immobilizing many types of antibodies in active states (Figure 13.7).

A recent study explored the effects of some of the above-described methods of antibody attachment on analyte binding, and found that certain immobilization approaches can increase analyte binding capacity up to 10-fold [66]. Thus, for nanoarray-type applications requiring high sensitivity and low detection limits, such directed protein immobilization techniques are likely to significantly improve their performance in cell-based or immunobased assays.

13.3.2 Bio-Analytical Applications

There can be significant benefits to the miniaturization of chip-based protein assays. These benefits include the use of less capture materials, less analyte, a reduction in the total sample volume and, under certain circumstances, lower limits of detection over conventional immunoassays. Although these nanopatterning techniques are still in their infancy, they represent the next major step in the miniaturization of immunoassays.

A proof-of-concept example of this type of diagnostic application was recently carried out by our group in collaboration with the group of Wolinsky [20], where nanoarrays of monoclonal antibodies for HIV-1 p24 were utilized to detect HIV-1 p24 antigen in blood samples (1 μL) obtained from men with fewer than 50 copies of RNA per mL of plasma (Figure 13.8). The presence of the array-captured p24 was measured by AFM, and the signal was amplified by treating the array

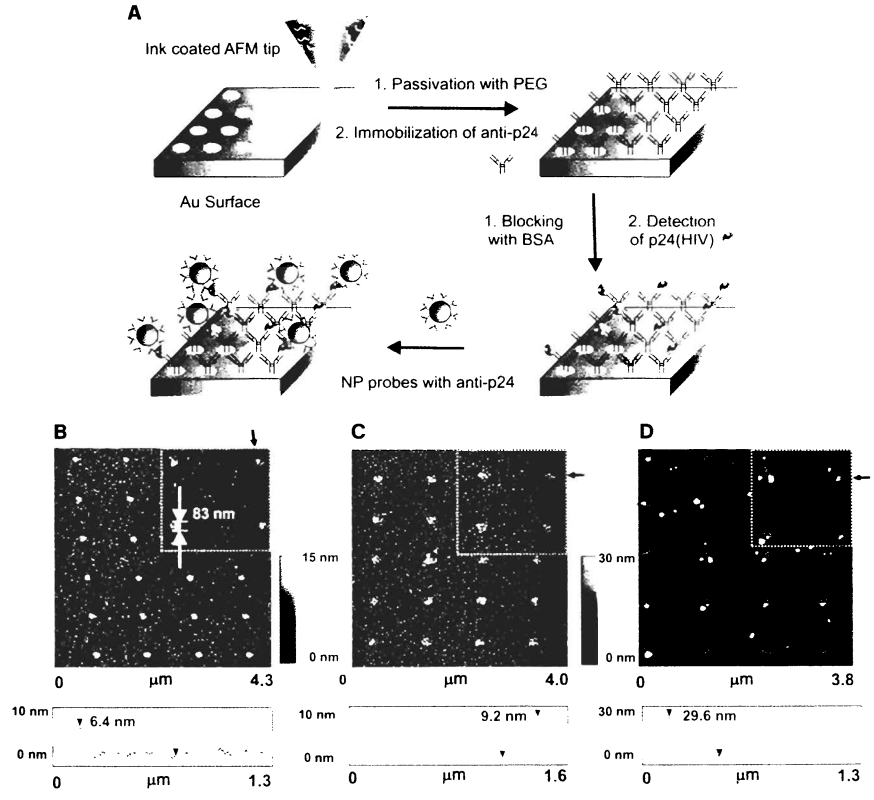

Fig. 13.8 (A) Schematic representation of the detection of HIV-1 p24 through the use of antibody nanoarrays. AFM images and height profiles for (B) an anti-p24 nanoarray (6.4 ± 0.9 nm; n = 10) adsorbed on MHA, (C) after p24 binding (height increase of 2.3 ± 0.6 nm; n = 10), and (D) detection and amplification of p24 through a sandwich complex with anti-p24 coated gold NPs (height increase of 20.3 ± 1.9 nm; n = 10). (Reprinted with permission from Ref. [20]; © 2004, American Chemical Society.)

with captured target with anti-p24-modified Au NPs, allowing for a significant increase in the height of the spots. This nanoarray-based assay exhibited a limit of detection (0.025 pg mL^{-1}) – three orders of magnitude lower than the conventional enzyme-linked immunosorbent assay (ELISA), with a detection limit of 5 pg mL^{-1}.

13.3.3
Dynamic and Motile Nanoarrays

Chip-based capture and release of target proteins directly from complex mixtures, in the context of nanoarrays, could provide functionality in integrated bioanalytical nanoscale devices in which the transport, separation, and detection of a small number of biomolecules could be performed in one integrated system. Chilkoti, Zauscher, and coworkers [21] have fabricated stimulus-responsive elastin-like polypeptide (ELP) nanostructures that respond to changes in ionic strength and temperature. ELP nanostructures were covalently end-grafted onto 200-nm features of ω-substituted alkane thiolates generated by DPN. A thioredoxin–ELP fusion protein was immobilized onto these ELP nanopatterns above the lower critical solution temperature (LCST). Below the LCST, the thioredoxin could be released back into solution. These experiments demonstrate that "smart," surface-confined biomolecular switches can be built and integrated into nanoscale bioanalytical devices.

Another type of dynamic protein nanoarray has been used in the development of a hybrid nanodevice based on a rotary motor. Soong et al. [67] demonstrated that a multi-subunit protein complex (ATP synthase) with domains that rotate about its membrane-bound axis during the hydrolysis of ATP, could be used to power the rotation of an inorganic Ni rod (nanopropeller) (Figure 13.9). Ni posts, 200 nm in height and 80 nm in diameter, were fabricated by electron-beam lithography. These arrays were subsequently treated with a thermostable form of the F_1-ATPase, with a 10× histidine tag engineered into the β-subunit coding sequence. Finally, biotinylated coated Ni rods were allowed to specifically attach to the lever (streptavidin conjugate) on the γ-subunit of the F_1-ATPase. In the presence of ATP, the nanodevice exhibited an endurance cycle of ~2.5 h. Despite the fact that the fabrication yield was low, once optimized, this type of functional dynamic nanoarray might be used to build integrated biomolecular motors with nanoengineered systems to produce nanomechanical devices.

13.3.4
Cell-Surface Interactions

Cellular adhesion is a process mediated by the interaction of cell-surface receptors (i.e., integrin) with ligands from the extracellular matrix (ECM), which results in the clustering of these receptors into focal adhesion complexes. This elaborate and highly regulated process is believed to play a significant role in many essential cellular functions (e.g., motility, proliferation, differentiation, and apoptosis)

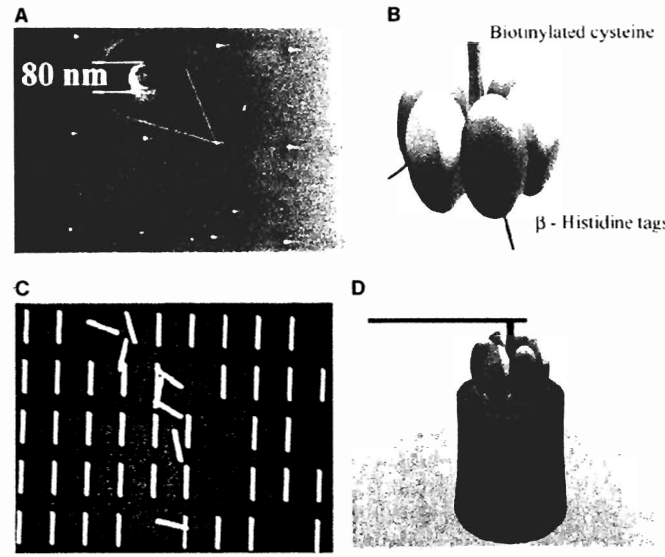

Fig. 13.9 (A) Schematic diagram of the F_1-ATPase biomolecular motor-powered nanomechanical device. The device consisted of (A) a Ni post (200 nm height, 80 nm diameter), (B) the F_1-ATPase biomolecular motor, and (C) a nanopropeller (length 750–1400 nm, diameter 150 nm). The device (D) was assembled using sequential additions of individual components and different attachment chemistries. (Reprinted with permission from Ref. [67]; © 2000, American Association for the Advancement of Science.)

[68, 69]. Most studies involving the signaling of focal adhesion complexes with surface-immobilized proteins have involved structures made by conventional microfabrication techniques. These studies have been limited to single-component protein arrays, typically generated by indirect robotic spotting and μCP methods [1, 70, 71]. Recently, researchers have begun to explore how protein arrays fabricated by techniques that offer high resolution can be used to probe surface cellular interactions, and some of these advances are summarized below.

Our group, in collaboration with group of Mrksich, has utilized DPN to generate patterns of retronectin features as small as 200 nm with 700 nm separation distances [6]. Cells were found to adhere and spread, exclusively, on the nanopatterned regions. The cellular morphology was found to be a direct consequence of the sizes and spacings of the patterned protein. These studies were the first to demonstrate that protein structures, well below 1 μm in size, can support cell adhesion.

Since then, others have used novel block copolymer-based strategies to fabricate peptide arrays for probing the feature size dependence in cell adhesion. These experiments were carried out in the context of the RGDfk adhesion peptide (see

Section 13.2.5) [51]. The features in these patterns were designed to be small enough (dot diameter < 8 nm) to capture a single integrin protein per dot. From these studies, Spatz and coworkers [51] have concluded that local dot-to-dot separation, rather than global dot density, is critical for inducing cell adhesion and focal adhesion assembly. A separation of ≥ 73 nm between adhesive dots resulted in limited cell attachment and spreading, and dramatically reduced the formation of focal adhesion and actin stress fibers.

Protein nanoarrays have been used to explore how the number, availability, and distribution of fibronectin (an ECM protein) features can dictate the shape and mobility of a cell. Lehnert et al. [72] utilized μCP and nCP techniques to generate patterns of fibronectin where the feature size was varied from the micro- to nanoscale, while keeping the dot-to-dot spacing constant. When the dot-to-dot spacing was less than 5 μm, cells cultured on these substrates could adhere and spread on fibronectin features as small as 0.1 μm^2. However, when the dot spacing was systematically altered over a range of 5 to 25 μm, the cells exhibited binding and adopted unusual shapes, depending on the type of fibronectin pattern (Figure 13.10). Finally, the ability of cells to spread and migrate on these patterns ceased when the dot-to-dot separation exceeded 30 μm. Therefore, the results of these experiments suggest that the extent of cell spreading is directly correlated to the substratum coverage of fibronectin, and not the geometrical pattern.

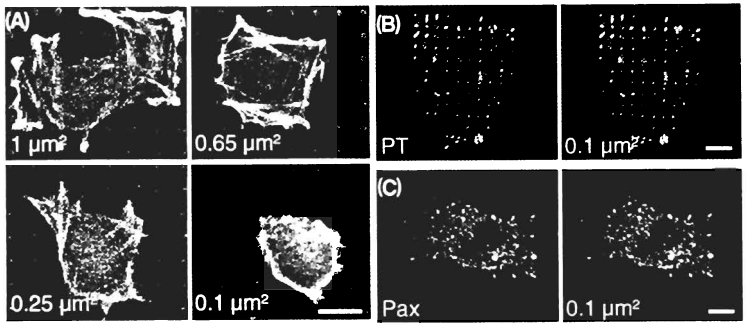

Fig. 13.10 Fibronectin arrays comprising dots of 0.1 μm^2 induce intracellular signaling, but do not support cell spreading at distances >5 μm. (A) B16 cells growing on fibronectin arrays with varying dot sizes (as indicated in lower left corner) and with a constant spacing of 5 μm (center-to-center). Cells spreading and the formation of actin stress fibers could be observed on dots down to 0.25 μm^2. However, dots of 0.1 μm^2 adhered but did not spread. Scale bar = 10 μm. (B) A cell sitting on 0.1 μm^2 dots with 2-μm spacing. Phosphotyrosine (PT, green) accumulates in areas of the cell overlying fibronectin dots (red), indicating that an area of 0.1 μm^2 is sufficient to induce intracellular signaling. (C) Staining for paxilin (Pax, green) of a cell sitting on 0.1 μm^2 fibronectin dots (red) separated by distances of 4 μm. Scale bar = 5 μm. (Reprinted with permission from Ref. [72]; © 2004, The Company of Biologists.)

13.4
DNA Nanoarrays

Although few studies have been conducted to date regarding the development of DNA nanoarrays, such highly miniaturized structures could be quite useful in developing new diagnostic systems that require small sample volumes, and also in controlling the assembly of material building blocks with complementary oligonucleotides. In nanosystems, there is often a need to control the positioning of building blocks at the single particle level in the context of higher-ordered, larger structures. Alternatively, there may be a need to immobilize such building blocks at specific sites in an integrated device in such a way that allows such structures to be addressed macroscopically. Because the chemical recognition properties of DNA can be tailored by virtue of its sequence, DNA represents the ideal building block for creating chemical affinity templates with nanoscopic features that have highly tailorable recognition properties. In this regard, it has been shown that DNA features can be made as small as 50 nm, and the oligonucleotides used in orthogonal assembly approaches, where each feature can be designed to recognize a specific type of building block and immobilize it at a specific location on a substrate [73]. For a 15-mer recognition sequence, there are 4^{15} unique chemical codes. Not all of these are non-overlapping in terms of their recognition properties, but many of them are and so can be selectively used for different assembly applications. Proof-of-concept orthogonal assembly has been demonstrated with DNA nanoarrays and oligonucleotide-modified Au NPs [7, 73]. The assembly strategy has been used in the context of nanoarrays to fabricate unusual single-particle electronic devices [19] and functional bioactive arrays for protein diagnostics [20]. These early advances are briefly discussed in Sections 13.4.2 and 13.4.3.

13.4.1
Strategies for Preparing DNA Nanoarrays

In contrast to the chemistry used to immobilize proteins (see Section 13.3.1), the approach used to immobilize DNA in the context of nanoarrays is almost identical to what has been used with microarrays. The immobilization of DNA on surfaces can be achieved either in a single step or in multiple steps, depending on the nature of the surface functional groups and whether or not the DNA is chemically modified with functional groups that can direct its immobilization. In this section, we will discuss the various immobilization chemistries reported in the literature for generating DNA nanoarrays.

In the simplest approach, DNA can be patterned using electrostatic interactions between a surface and unmodified DNA. At neutral pH, DNA is negatively charged and the phosphate groups in the DNA backbone can bind strongly to a positively charged surface such as a poly-L-lysine-coated glass substrate [74]. Since immobilization occurs nonspecifically, it is often difficult to effect hybridization to complementary targets, and this has been a major drawback with this approach.

One of the attributes of DNA is that it can be chemically modified with functional groups on its 3′ or 5′ ends. Indeed, one of the most widely used immobilization methods utilizes 3′ or 5′ alkylthiol-modified DNA. Such oligonucleotides will readily adsorb onto gold surfaces [7, 48], and this chemistry has been used to prepare nanoarrays by DPN. In this approach, there is a chemical interaction between the sulfur-containing appendage of the DNA and the gold surface to form what many believe to be a gold–thiolate bond [75]. In addition, Michael Addition chemistry can be used to immobilize 5′ acrylamide-modified oligonucleotides [7] on oxide substrates that have been pre-modified with a 3′-mercaptopropyltrimethoxysilane (MPTMS) layer [76]. Recently, Yu and coworkers [47] have generated nanoarrays of DNA on poly(methyl methacrylate) (PMMA) substrates using a covalent immobilization strategy. The PMMA surface was initially activated to generate surface aldehyde groups that react with 5′ amine-modified DNA [77]. In another useful strategy, our group [73] initially patterned 16-mercaptohexadecanoic acid (MHA) on a gold surface and activated the terminal carboxyl moieties with 1-ethyl-3-(3-dimethylaminopropyl) carbodiimide hydrochloride (EDC). 5′-Alkylamine-modified DNA is then coupled to the activated MHA, and this results in the formation of an amide bond [73]. The biotin–streptavidin interaction also has been used as an immobilization modality for DNA. For example, biotinylated DNA has been immobilized onto streptavidin-coated glass surfaces to generate oligonucleotide nanopatterns [30, 32].

13.4.2
DNA-Based Schemes for Biodetection

DNA nanoarrays are just beginning to be explored for their potential in diagnostics. One of the issues pertaining to their utility is the challenge associated with readout. With extraordinarily small features spaced sub-300 nm apart, it is difficult to use conventional optical methods such as fluorescence microscopy to monitor probe-target-array binding events. However, when the feature size of an individual pattern is miniaturized down to the length scale of the DNA structures being probed, the physical properties of that feature – including the height, shape, and hydrophobicity – change substantially upon binding. In addition, an entire array can be built within the field of view of a conventional scanning probe microscope ($100 \times 100\ \mu M$). This allows a variety of scanning probe-based methods to be used, though these are impractical for microarrays because of the large area that must be interrogated, as readout mechanisms for following nanoarray binding events.

We have demonstrated this concept, in part, by preparing nanoarrays of oligonucleotides by DPN [7, 73]. In this case, the feature spacing was not particularly small, and consequently fluorophore-labeled probes and fluorescence could be used, as well as NP probes [78] and AFM to monitor and study the sequence-specific hybridization events (see Figure 13.3). With the advent of massively parallel writing and multi-ink capabilities, DPN has the throughput to generate highly miniaturized DNA chips with extraordinary chemical complexity. Before this capability becomes a practical reality, inking strategies must be developed as well as methods for on-chip, *in-situ* synthesis of the DNA in the context of a DPN experiment.

In addition to the optical and scanning readout of nanoarrays, electrical readout has been preliminarily explored. In this regard, nanoelectrodes have been prepared with gaps selectively functionalized with different oligonucleotides. In this configuration, once the functionalized gaps have hybridized with a target, the area with NP probes can be further developed and the transport properties of the functionalized gap measured [19]. This approach allows the electrical transport properties of particles to be studied down to the single-particle level, and also provides for an on-off readout mechanism for the array in the context of detection.

13.4.3
Applications of Rationally Designed, Self-Assembled 2-D DNA Nanoarrays

DNA tile lattices have been used to construct periodic arrays of well-defined nanostructures from simple oligonucleotide building blocks [79]. Recently, hybridization strategies have been used to assemble NPs, conjugated to single-stranded DNA molecules, into chain-like structures. Mao et al. generated 1-D arrays of Au NPs by combining DNA-encoded self-assembly with rolling-circle polymerization [80]. These arrays, in certain cases, were several micrometers in length. Yan and coworkers [52, 53] demonstrated the incorporation of a single Au NP into a rationally designed DNA-nanostructured building block, where they used NP-bearing DNA tiles for the directed assembly of 2-D NP arrays with periodic square-like configurations and precisely controlled interparticle spacings. This square arrangement of NPs has been considered as a potential tool for constructing novel cellular nonlinear logic networks [81, 82].

The precise control of periodic spacing between proteins has been demonstrated by using DNA nanoarrays generated by programmed self-assembly. Park et al. demonstrated the ability to generate periodic protein arrays through the use of templated self-assembly of streptavidin onto each DNA tile containing a biotinylated group terminal to the oligonucleotides (Figure 13.11) [83]. Fully programmable DNA-templated protein nanoarrays, where proteins can be positioned with precision and specificity, might allow functional protein templates with nanometer dimensions to be built for single molecule detection. More recently, LaBean and coworkers [59] developed a fully addressable, finite-sized DNA nanoarray displaying a variety of programmed patterns by using a novel stepwise hierarchical assembly technique. In order to properly address the nanoarrays, these authors included loop strands modified with biotin at desired points in the assembly process, and probed the binding of streptavidin at biotinylated sites (see Figure 13.6).

The use of aptamers in self-assembled DNA nanoarrays has been used as a robust platform specifically to attach proteins in periodic arrangements. Aptamers are relatively small RNA or DNA sequences that can be selected through a pro-

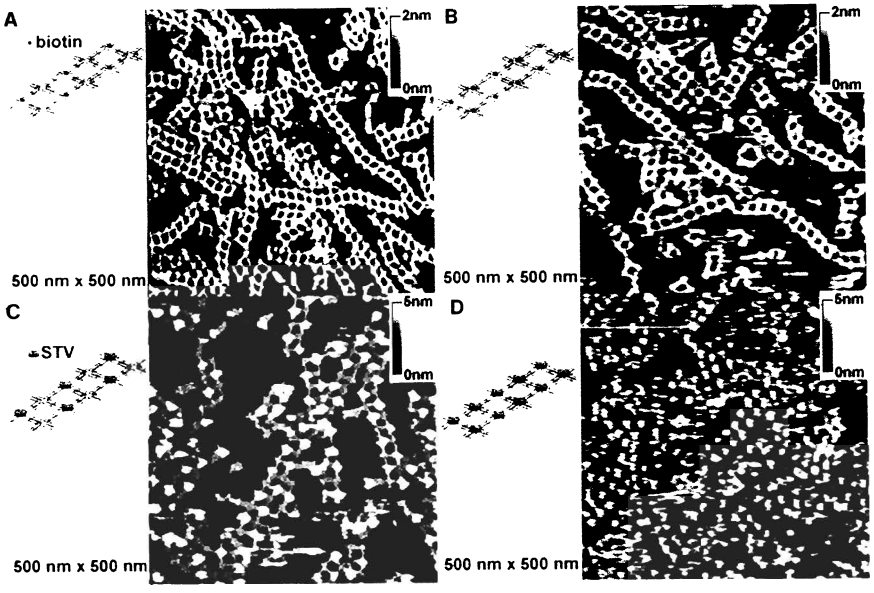

Fig. 13.11 AFM images of the results of programmed assembly of streptavidin on 1-D DNA nanotiles. (A, B) AFM images of bare A*B and A*B* nanotiles before streptavidin binding, respectively. (C, D) AFM images of A*B and A*B* nanotiles after streptavidin binding. (Reprinted with permission from Ref. [83]; © 2005, American Chemical Society.)

cess called SELEX from random pools, based on their ability to bind a specific protein and or small molecule. Leu et al. first showed how a DNA aptamer could be used in the rational design of DNA nanostructures for the directed assembly of thrombin [84]. Thrombin binding indicates that the thrombin-binding aptamer still functions as the protein-binding moiety upon incorporation into a complex DNA architecture. Aptamer-directed self-assembly of proteins on DNA nanotemplates would allow the relative positions of proteins to be changed in real time, which could enable the study of proximity effects on protein–protein interactions.

In addition to use as directing groups in forming complex NP and protein arrays, self-assembled DNA nanoarrays also have been used as molecular masks in lithographic experiments [85]. In such experiments, the desired DNA nanostructures are generated on a mica substrate, and then used as a mask to control metal deposition. Removal of the DNA mask from the substrate yields a negative replica of the DNA nanostructure. 1-D and 2-D metallic nanopatterns with feature sizes as small as ~10 nm have been generated by this method, though it is possible to create complex structures with more sophisticated DNA motifs [86].

13.5
Virus Nanoarrays

High-resolution nanolithographic techniques allow biological structures to be manipulated at the single-particle level. Although this cannot yet be done routinely with structures as small as proteins, it is possible to manipulate entities such as viruses at this level. The first example of such control involved the use of DPN-generated affinity templates to immobilize tobacco mosaic virus particles (TMV, length = 300 nm, diameter = 18 nm) with excellent control over their orientation and spacing (Figure 13.12) [4]. In these studies, metal ion affinity templates of Zn(II), coordinated to MHA, that bind the natural carboxylate-rich surface moieties of TMV particles were used. Previously, our group [22] and others [23] had generated nanopatterns of NHS-terminated alkanethiols that covalently couple to genetically modified forms of the cow-pea mosaic virus (CPMV) presenting unnatural binding sites (i.e., cystine). However, CPMV particles (diameter = 30 nm) were too small to be isolated and studied at the single-particle level. With the state of the current DPN technology, virus particles 50 nm or larger in diameter are ideal for site-isolation.

Although the above-mentioned methods are very efficient for the immobilization of virus particles with well-known surface chemistries, there are other virus particles of interest that require another strategy. One such strategy has been through the use of antibodies that can recognize and capture surface proteins from a specific virus particle. Our group has reported an antibody immobilization scheme, utilizing metal ion affinity templates that yield active antibody arrays, for

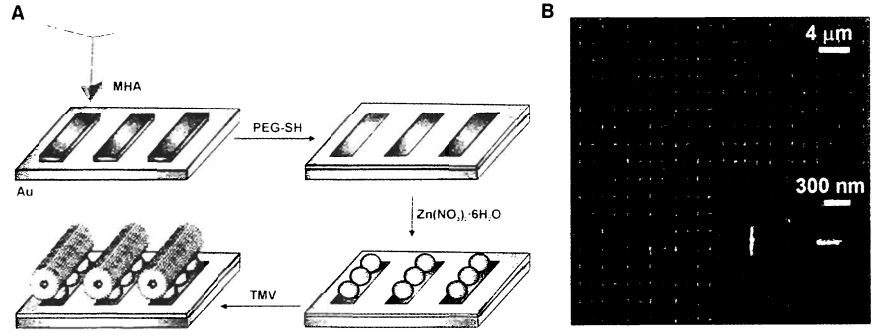

Fig. 13.12 (A) Schematic diagram depicting the process for generating 16-mercaptohexadecanoic acid (MHA) nanotemplates by DPN that were subsequently treated with $Zn(NO_3)_2 \cdot 6H_2O$ for the selective immobilization of single virus particles. (B) AFM tapping mode images of a perpendicular array (40 × 40 μm) of single tobacco mosaic virus (TMV) particles collected at a scan rate of 0.5 Hz. (Reprinted with permission from Ref. [4]; © 2006, Wiley-VCH.)

influenza and simian virus particles [24]. Currently, these surface-immobilized virus particles are being used to study how the number of virus particles, orientation, and presentation (i.e., neutralized) affect cell infectivity at the single-cell and/or single-virus particle level.

13.6 Outlook

Although, at present, we are still in the very early stages of developing ways of making and using bionanoarrays, some very significant advances have been made. Today, it is possible to use techniques such as DPN for the routine fabrication of certain classes of nanoarrays (e.g., one- or two-component structures over larger areas), and we are beginning to learn how to use such arrays to address issues in biology that cannot be addressed with their larger microarray counterparts. The small feature sizes in these arrays are providing research groups with the ability to manipulate biological structures at the single-particle level and to study multivalency in the context of cell-surface interactions. These tools have the potential to revolutionize many aspects of biology, including methods of probing and understanding viral infectivity and proliferation, cellular metabolic and signaling events, and general clinical diagnostics. However, in order to realize their full potential, methods must be developed that allows structures to be built routinely over large areas, with the ability to control feature size, shape, and composition on the sub-100 nm length scale. In particular, these techniques must be developed with biologists in mind, as they are less interested in how a bionanoarray is made but rather how to gain access to it and to acquire control over the structural parameters that make it functional and useful for their studies. Thus, it is imperative that an infrastructure be developed in this field that allows such structures to be built on demand, and in an automated manner. With the advent of high-resolution and massively parallel techniques such as DPN, this goal is achievable in the not-too-distant future.

References

1 Miller, U. R., Nicolau, D. V. (2005) *Microarray Technology and Its Applications*. Springer, New York.

2 Piner, R. D., Zhu, J., Xu, F., Hong, S. H., Mirkin, C. A. (1999) 'Dip-pen' nanolithography. *Science* **283** 661–663.

3 Rosi, N. L., Mirkin, C. A. (2005) Nanostructures in biodiagnostics *Chem. Rev.* **105**, 1547–1562.

4 Vega, R. A., Maspoch, D., Salaita, K., Mirkin, C. A. (2005) Nanoarrays of single virus particles. *Angew. Chem. Int. Ed.* **44**, 6013–6015.

5 Binnig, G., Quate, C. F., Gerber, C. (1986) Atomic Force Microscope. *Phys. Rev. Lett.* **56**, 930–933

6 Lee, K. B., Park, S. J., Mirkin, C. A., Smith, J. C., Mrksich, M. (2002) Protein nanoarrays generated by dip-pen nanolithography. *Science* **295**, 1702–1705.

7 Demers, L. M., Ginger, D. S., Park, S. J., Li, Z., Chung, S. W., Mirkin, C. A. (2002) Direct patterning of modified oligonucleotides on metals and insulators by dip-pen nanolithography. *Science* **296**, 1836–1838.

8 Wadu-Mesthrige, K., Xu, S., Amro, N. A., Liu, G. Y. (1999) Fabrication and imaging of nanometer-sized protein patterns. *Langmuir* **15**, 8580–8583.

9 Gu, J. H., Yam, C. M., Li, S., Cai, C. Z. (2004) Nanometric protein arrays on protein-resistant monolayers on silicon surfaces. *J. Am. Chem. Soc.* **126**, 8098–8099.

10 Zhao, Z. Y., Banerjee, P. A., Matsui, H. (2005) Simultaneous targeted immobilization of anti-human IgG-coated nanotubes and anti-mouse IgG-coated nanotubes on the complementary antigen-patterned surfaces via biological molecular recognition. *J. Am. Chem. Soc* **127** 8930–8931

11 Ginger, D. S., Zhang, H., Mirkin, C. A. (2004) The evolution of dip-pen nanolithography. *Angew. Chem. Int Ed.* **43** 30–45

12 Lee, K. B., Lim, J. H., Mirkin, C. A. (2003) Protein nanostructures formed via direct-write dip-pen nanolithography. *J. Am. Chem. Soc* **125**, 5588–5589.

13 Lim, J. H., Ginger, D. S., Lee, K. B., Heo, J., Nam, J. M., Mirkin, C. A. (2003) Direct-write dip-pen nanolithography of proteins on modified silicon oxide surfaces. *Angew. Chem. Int. Ed.* **42**, 2309–2312

14 Nam, J. M., Han, S. W., Lee, K. B., Liu, X. G., Ratner, M. A., Mirkin, C. A. (2004) Bioactive protein nanoarrays on nickel oxide surfaces formed by dip-pen nanolithography. *Angew. Chem. Int. Ed.* **43**, 1246–1249.

15 Wilson, D. L., Martin, R., Hong, S., Cronin-Golomb, M., Mirkin, C. A., Kaplan, D. L. (2001) Surface organization and nanopatterning of collagen by dip-pen nanolithography. *Proc. Soc. Natl. Acad. Sci. USA* **98**, 13660–13664.

16 Jiang, H. Z., Stupp, S. I. (2005) Dip-pen patterning and surface assembly of peptide amphiphiles. *Langmuir* **21** 5242–5246.

17 Cho, Y., Ivanisevic, A. (2004) SiOx surfaces with lithographic features composed of a TAT peptide. *J. Phys. Chem. B* **108**, 15223–15228.

18 Hyun, J., Kim, J., Craig, S. L., Chilkoti, A. (2004) Enzymatic nanolithography of a self-assembled oligonucleotide monolayer on gold. *J. Am. Chem. Soc.* **126**, 4770–4771

19 Chung, S. W., Ginger, D. S., Morales, M. W., Zhang, Z. F., Chandrasekhar, V., Ratner, M. A., Mirkin, C. A. (2005) Top-down meets bottom-up: Dip-pen nanolithography and DNA-directed assembly of nanoscale electrical circuits. *Small* **1**, 64–69.

20 Lee, K. B., Kim, E. Y., Mirkin, C. A., Wolinsky, S. M. (2004) The use of nanoarrays for highly sensitive and selective detection of human immunodeficiency virus type 1 in plasma. *Nano Lett.* **4**, 1869–1872.

21 Hyun, J., Lee, W. K., Nath, N., Chilkoti, A., Zauscher, S. (2004) Capture and release of proteins on the nanoscale by stimuli-responsive elastin-like polypeptide 'switches' *J. Am. Chem. Soc.* **126**, 7330–7335.

22 Smith, J. C., Lee, K. B., Wang, Q., Finn, M. G., Johnson, J. E., Mrksich, M., Mirkin, C. A. (2003) Nanopatterning the chemospecific immobilization of cowpea mosaic virus capsid. *Nano Lett.* **3**, 883–886.

23 Cheung, C. L., Camarero, J. A., Woods, B. W., Lin, T. W., Johnson, J. E., De Yoreo, J. J. (2003) Fabrication of assembled virus nanostructures on templates of chemoselective linkers formed by scanning probe nanolithography. *J. Am. Chem. Soc.* **125**, 6848–6849.

24 Vega, R. A., Maspoch, D., Shen, C. K.-F., Kakkassery, J. J., Chen, B. J., Lamb, R. A., Mirkin, C. A. (2006) Functional antibody arrays through metal ion affinity templates. *ChemBioChem*. **7**, 1653–1657

25 Liu, M. Z., Amro, N. A., Chow, C. S., Liu, G. Y. (2002) Production of nanostructures of DNA on surfaces. *Nano Lett.* **2**, 863–867

26 Liu, G. Y., Amro, N. A. (2002) Positioning protein molecules on surfaces: A nanoengineering approach to supramolecular chemistry. *Proc. Soc. Natl. Acad. Sci. USA* **99**, 5165–5170.

27 Salaita, K., Lee, S. W., Wang, X. F., Huang, L., Dellinger, T. M., Liu, C., Mirkin, C. A. (2005) Sub-100 nm, centimeter-scale, parallel dip-pen nanolithography. *Small* **1**, 940–945.

28 Salaita, K., Wang, Y., Fragala, J., Vega, R. A., Liu, C., Mirkin, C. A. (2006) Massively parallel dip-pen nanolithography with 55.000-pen two-dimensional Arrays. *Angew. Chem. Int. Ed.* **45**, 7220–7223.

29 Hasnma, P. K., Drake, B., Marti, O., Gould, S. A., Prater, C. B. (1989) The scanning ion-conductance microscope. *Science* **243**, 641–643.

30 Bruckbauer, A., Ying, L. M., Rothery, A. M., Zhou, D. J., Shevchuk, A. I., Abell, C., Korchev, Y. E., Klenerman, D. (2002) Writing with DNA and protein using a nanopipet for controlled delivery. *J. Am. Chem. Soc.* **124**, 8810–8811.

31 Bruckbauer, A., Zhou, D. J., Ying, L. M., Korchev, Y. E., Abell, C., Klenerman, D. (2003) Multicomponent submicron features of biomolecules created by voltage controlled deposition from a nanopipet. *J. Am. Chem. Soc.* **125**, 9834–9839.

32 Rodolfa, K. T., Bruckbauer, A., Zhou, D. J., Korchev, Y. E., Klenerman, D. (2005) Two-component graded deposition of biomolecules with a double-barreled nanopipette. *Angew. Chem. Int. Ed.* **44**, 6854–6859.

33 Tseng, A. A., Chen, K., Chen, C. D., Ma, K. J. (2003) Electron beam lithography in nanoscale fabrication: recent development. *IEEE Trans. Electronics Packaging Manufactur.* **26**, 141–149.

34 Zhang, G. J., Tanii, T., Zako, T., Hosaka, T., Miyake, T., Kanari, Y., Funatsu, T. W., Ohdomari, I. (2005) Nanoscale patterning of protein using electron beam lithography of organosilane self-assembled monolayers. *Small* **1**, 833–837.

35 Zhang, G. J., Tanii, T., Funatsu, T., Ohdomari, I. (2004) Patterning of DNA nanostructures on silicon surface by electron beam lithography of self-assembled monolayer. *Chem. Commun.* **15**, 786–787.

36 Hu, W. C., Sarveswaran, K., Lieberman, M., Bernstein, G. H. (2005) High-resolution electron beam lithography and DNA nano-patterning for molecular QCA. *IEEE Trans. Nanotechnol.* **4**, 312–316.

37 Denis, F. A., Pallandre, A., Nysten, B., Jonas, A. M., Dupont-Gillain, C. C. (2005) Alignment and assembly of adsorbed collagen molecules induced by anisotropic chemical nanopatterns. *Small* **1**, 984–991.

38 Pallandre, A., De Meersman, B., Blondeau, F., Nysten, B., Jonas, A. M. (2005) Tuning the orientation of an antigen by adsorption onto nano-striped templates. *J. Am. Chem. Soc.* **127**, 4320–4325.

39 Falconnet, D., Pasqui, D., Park, S., Eckert, R., Schift, H., Gobrecht, J., Barbucci, R., Textor, M. (2004) A novel approach to produce protein nanopatterns by combining nanoimprint lithography and molecular self-assembly. *Nano Lett.* **4**, 1909–1914.

40 Hoff, J. D., Cheng, L. J., Meyhofer, E., Guo, L. J., Hunt, A. J. (2004) Nanoscale protein patterning by imprint lithography. *Nano Lett.* **4**, 853–857.

41 Xia, Y. N., Whitesides, G. M. (1998) Soft lithography. *Annu. Rev. Mater. Sci.* **28**, 153–184.

42 Renaultt, J. P., Bernard, A., Bietsch, A., Michel, B., Bosshard, H. R., Delamarche, E., Kreiter, M., Hecht, B., Wild, U. P. (2003) Fabricating arrays of single protein molecules on glass using microcontact printing. *J. Phys. Chem. B* **107**, 703–711.

43 Li, H. W., Muir, B. V. O., Fichet, G., Huck, W. T. S. (2003) Nanocontact printing: A route to sub-50-nm-scale chemical and biological patterning. *Langmuir* **19**, 1963–1965.

44 Gerding, J. D., Willard, D. M., Van Orden, A. (2005) Single-feature inking and stamping: A versatile approach to molecular patterning. *J. Am. Chem. Soc.* **127**, 1106–1107.

45 Mirkin, C. A., Demers, L. M., Ginger, D. S. (2003) Patent WO-2003048314.1-76: PCT/US2002/038252.

46 Lin, H. H., Sun, L., Crooks, R. M. (2005) Replication of a DNA microarray. *J. Am. Chem. Soc.* **127**, 11210–11211.

47 Yu, A. A., Savas, T., Cabrini, S., diFabrizio, E., Smith, H. I., Stellacci, F. (2005) High resolution printing of DNA feature on poly(methyl methacrylate) substrates using supramolecular nano-stamping. *J. Am. Chem. Soc.* **127**, 16774–16775.

48 Yu, A. A., Savas, T. A., Taylor, G. S., Guiseppe-Elie, A., Smith, H. I., Stellacci, F. (2005) Supramolecular nanostamping: Using DNA as movable type. *Nano Lett.* **5**, 1061–1064.

49 Denis, F. A., Hanarp, P., Sutherland, D. S., Dufrene, Y. F. (2004) Nanoscale chemical patterns fabricated by using colloidal lithography and self-assembled monolayers. *Langmuir* **20**, 9335–9339.

50 Pammer, P., Schlapak, R., Sonnleitner, M., Ebner, A., Zhu, R., Hinterdorfer, P., Hoglinger, O., Schindler, H., Howorka, S. (2005) Nanopatterning of biomolecules with microscale beads. *ChemPhysChem.* **6**, 900–903.

51 Arnold, M., Cavalcanti-Adam, E. A., Glass, R., Blummel, J., Eck, W., Kantlehner, M., Kessler, H., Spatz, J. P. (2004) Activation of integrin function by nanopatterned adhesive interfaces. *ChemPhysChem.* **5**, 383–388.

52 Sharma, J., Chhabra, R., Liu, Y., Ke, Y. G., Yan, H. (2006) DNA-templated self-assembly of two-dimensional and periodical gold nanoparticle arrays. *Angew. Chem. Int. Ed.* **45**, 730–735.

53 Zhang, J. P., Liu, Y., Ke, Y. G., Yan, H. (2006) Periodic square-like gold nanoparticle arrays templated by self-assembled 2D DNA nanogrids on a surface. *Nano Lett.* **6**, 248–251.

54 Cai, Y. G., Ocko, B. M. (2005) Large-scale fabrication of protein nanoarrays based on nanosphere lithography. *Langmuir* **21**, 9274–9279.

55 Haynes, C. L., Van Duyne, R. P. (2001) Nanosphere lithography: A versatile nanofabrication tool for studies of size-dependent nanoparticle optics. *J. Phys. Chem. B* **105**, 5599–5611.

56 Hulteen, J. C., Treichel, D. A., Smith, M. T., Duval, M. L., Jensen, T. R., Van Duyne, R. P. (1999) Nanosphere lithography: size-tunable silver nanoparticle and surface cluster arrays. *J. Phys. Chem. B* **103**, 3854–3863.

57 Haes, A. J., Chang, L., Klein, W. L., Van Duyne, R. P. (2005) Detection of a biomarker for Alzheimer's disease from synthetic and clinical samples using a nanoscale optical biosensor. *J. Am. Chem. Soc.* **127**, 2264–2271.

58 Liu, Y., Ke, Y. G., Yan, H. (2005) Self-assembly of symmetric finite-size DNA nanoarrays. *J. Am. Chem. Soc.* **127**, 17140–17141.

59 Park, S. H., Pistol, C., Ahn, S. J., Reif, J. H., Lebeck, A. R., Dwyer, C., LaBean, T. H. (2006) Finite-size, fully addressable DNA tile lattices formed by hierarchical assembly procedures. *Angew. Chem. Int. Ed.* **45**, 735–739.

60 MacBeath, G., Schreiber, S. L. (2000) Printing proteins as microarrays for high-throughput function determination. *Science* **289**, 1760–1763.

61 Chen, S., Liu, L., Zhou, J., Jiang, S. (2003) Controlling antibody orientation on charged self-assembled monolayers. *Langmuir* **19**, 2859–2864.

62 Zull, J. E., Reed-Mundell, J., Lee, Y. W., Vezenov, D., Ziats, N. P., Anderson, J. M., Sukenik, C. N. (1994) Problems and approaches in covalent attachment of peptides and proteins to inorganic surfaces for biosensor applications. *J. Indust. Microbiol. Biotechnol.* **13**, 137–143.

63 Babacam, S., Pivarnik, P., Lecther, S., Rand, A. G. (2000) Evaluation of antibody immobilization methods for piezoelectric biosensor application. *Biosensors Bioelectron.* **15**, 615–621.

64 Lee, S. W., Oh, B.-K., Sanedrin, R. G., Salaita, K., Fujigaya, T., Mirkin, C. A.

(2006) Biologically active protein nanoarrays generated using parallel dip-pen nanolithography. *Adv. Mater.* **18**, 1133–1136.

65 Lynch, M., Mosher, C., Huff, J., Nettikadan, S., Johnson, J., Henderson, E. (2004) Functional protein nanoarrays for biomarker profiling. *Proteomics* **4**, 1695–1702.

66 Peluso, P., Wilson, D. S., Do, D., Tran, H., Venkatasubbaiah, M., Quincy, D., Heidecker, B., Poindexter, K., Tolani, N., Phelan, M. (2003) Optimizing antibody immobilization strategies for the construction of protein microarrays. *Anal. Biochem.* **312**, 113–124.

67 Soong, R. K., Bachand, G. D., Neves, H. P., Olkhovets, A. G., Craighead, H. G., Montemagno, C. D. (2000) Powering an inorganic nanodevice with a biomolecular motor. *Science* **290**, 1555–1558.

68 Blau, H. M., Baltimore, D. (1991) Differentiation requires continuous regulation. *J. Cell Biol.* **112**, 781–783.

69 Ruoslahti, E., Obrink, B. (1996) Common principles in cell adhesion. *Exp. Cell Res.* **227**, 1–11.

70 Chen, C. S., Mrksich, M., Hung, S., Whitesides, G. M., Ingber, D. E. (1997) Geometric control of cell life and death. *Science* **276**, 1425–1428.

71 Shim, J., Bersano-Begey, T. F., Zhu, X. Y., Tkaczyk, A. H., Linderman, J. J., Takayama, S. (2003) Micro- and nanotechnologies for studying cellular function. *Curr. Topics Med. Chem.* **3**, 687–703.

72 Lehnert, D., Wehrle-Haller, B., David, C., Weiland, U., Ballestrem, C., Imhof, B. A., Bastmeyer, M. (2004) Cell behaviour on micropatterned substrata: limits of extracellular matrix geometry for spreading and adhesion. *J. Cell Sci.* **117**, 41–52.

73 Demers, L. M., Park, S. J., Taton, T. A., Li, Z., Mirkin, C. A. (2001) Orthogonal assembly of nanoparticle building blocks on dip-pen nanolithographically generated templates of DNA. *Angew. Chem. Int. Ed.* **40**, 3071–3073.

74 Tabata, H., Uno, T., Ohtake, T., Kawai, T. (2005) DNA patterning by nano-imprinting technique and its application for bio-chips. *J. Photopolymer Sci. Technol.* **18**, 519–522.

75 Bain, C. D., Troughton, E. B., Tao, Y. T., Evall, J., Whitesides, G. M., Nuzzo, R. G. (1989) Formation of monolayer films by the spontaneous assembly of organic thiols from solution onto gold. *J. Am. Chem. Soc.* **111**, 321–335.

76 Kurth, D. G., Bein, T. (1993) Surface reactions on thin layers of silane coupling agents. *Langmuir* **9**, 2965–2973.

77 Fixe, F., Dufva, M., Telleman, P., Christensen, C. B. V. (2004) Functionalization of poly(methyl methacrylate) (PMMA) as a substrate for DNA microarrays. *Nucleic Acids Res.* **32**, e9.

78 Mirkin, C. A., Letsinger, R. L., Mucic, R. C., Storhoff, J. J. (1996) A DNA-based method for rationally assembling nanoparticles into macroscopic materials. *Nature* **382**, 607–609.

79 Winfree, E., Liu, F. R., Wenzler, L. A., Seeman, N. C. (1998) Design and self-assembly of two-dimensional DNA crystals. *Nature* **394**, 539–544.

80 Deng, Z. X., Tian, Y., Lee, S. H., Ribbe, A. E., Mao, C. D. (2005) DNA-encoded self-assembly of gold nanoparticles into one-dimensional arrays. *Angew. Chem. Int. Ed.* **44**, 3582–3585.

81 Yang, T., Kiehl, R. A., Chua, L. O. (2001) Tunneling phase logic cellular nonlinear networks. *Int. J. Bifurcation Chaos* **11**, 2895–2912.

82 Xiao, S., Liu, F., Rosen, A. E., Hainfeld, J. F., Seeman, N. C., Musier-Forsyth, K., Kiehl, R. A. (2002) Self-assembly of metallic nanoparticle arrays by DNA scaffolding. *J. Nanoparticle Res.* **4**, 313–317.

83 Park, S. H., Yin, P., Liu, Y., Reif, J. H., LaBean, T. H., Yan, H. (2005) Programmable DNA self-assemblies for nanoscale organization of ligands and proteins. *Nano Lett.* **5**, 729–733.

84 Liu, Y., Lin, C. X., Li, H. Y., Yan, H. (2005) Aptamer-directed self-assembly of protein arrays on a DNA nanostructure. *Angew. Chem. Int. Ed.* **44**, 4333–4338.

85 Deng, Z. X., Mao, C. D. (2004) Molecular lithography with DNA nanostructures. *Angew. Chem. Int. Ed.* **43**, 4068–4070.

86 Mao, C. D., LaBean, T. H., Reif, J. H., Seeman, N. (2000) Logical computation using algorithmic self-assembly of DNA triple-crossover molecules (2000). *Nature* **407**, 750–750.